Circular states of atomic hydrogen

Robert Lutwak,* Jeffrey Holley, Pin Peter Chang, Scott Paine,† and Daniel Kleppner
Department of Physics and Research Laboratory of Electronics, Massachusetts Institute of Technology, Cambridge, Massachusetts 02139

Theodore Ducas
Department of Physics, Wellesley College, Wellesley, Massachusetts 02181
(Received 21 Februrary 1997)

We describe the creation of circular states of hydrogen by adiabatic transfer of a Rydberg state in crossed electric and magnetic fields, and also by adiabatic passage in a rotating microwave field. The latter method permits rapid switching between the two circular states of a given n manifold. The two methods are demonstrated experimentally, and results are presented of an analysis of the field ionization properties of the circular states. An application for the circular states is illustrated by millimeter-wave resonance in hydrogen of the $n=29\rightarrow n=30$ transition. [S1050-2947(97)00608-2]

PACS number(s): 32.80.Rm, 32.30.Bv, 06.20.Jr

I. INTRODUCTION

Rydberg states of an atom which have the maximum value of $|m|$ are known as circular states because the excited electron's behavior approaches the classical limit of localized motion in a circular orbit. Specifically, $|m|=l=n-1$, where n,l,m are the familiar principal and spherical quantum numbers, and, for a Rydberg atom, $n\gg 1$. Within each manifold of states with principal quantum number n, there are two such states with $m=\pm(n-1)$. Circular states exhibit extraordinarily long radiative lifetimes because they can decay only in a single channel to the next lower circular state. The lifetimes scale as n^5, in contrast to those of low angular momentum states which scale as n^3. Circular states exhibit no first-order Stark shift and their second-order shift is the smallest for all states of a given n. The circular state wave function is localized far from the nucleus. Consequently, energy-level corrections for nuclear structure and QED effects are extremely small. Because of these properties, circular states have found applications in cavity quantum electrodynamics [1–4], metrology [5–7], collisions [8], and intense radiation field dynamics [9].

Circular states have been produced in most of the alkali metals and in barium, but not, to date, in atomic hydrogen, which involves some special challenges. The initial stage of the process, exciting a hydrogen atom to a low-$|m|$ Rydberg state, is difficult because intense UV laser sources are required. More seriously, the high degeneracy of hydrogen complicates the transfer process.

Circular states cannot be directly populated from the ground state by laser excitation because only one unit of angular momentum can be transferred per photon. Consequently, circular state production involves first exciting an optically allowed low-$|m|$ Rydberg state and then transferring the population to one of the $|m|=(n-1)$ circular states. Three approaches have been employed for providing the required angular momentum: adiabatic microwave transfer, which involves absorption of microwave photons as a Stark field is adiabatically decreased [10]; a method in which the atoms are excited in a circularly polarized microwave field which is subsequently turned off adiabatically [11]; and the crossed fields method, in which a low-$|m|$ Stark state is transformed into a circular state by adiabatic redefinition of the quantization basis [12]. The choice of production technique depends to some extent on the atomic structure, particularly on perturbations to the low-$|m|$ states in Rydberg atoms other than hydrogen, and also on the experimental application for the atoms. In this paper we describe production of circular states of hydrogen using both adiabatic microwave transfer and the crossed fields method.

The intended application for circular states of hydrogen is a precision measurement of the Rydberg frequency cR_{H} by millimeter-wave spectroscopy of the $n=29\rightarrow n=30$ transition (at 256 GHz) between circular states. For these transitions, $\Delta m=\pm 1$, and there is a first-order Zeeman effect. This can be eliminated by alternately exciting the $\Delta m=+1$ and $\Delta m=-1$ transitions. Thus it is essential to be able to excite selectively either the $m=n-1$ or the $m=-(n-1)$ circular state.

As background to this work, we briefly summarize the history of circular state production. Hulet and Kleppner created circular states in 1983 by adiabatic microwave transfer in lithium [10]. In this method, the atoms are transferred from a low-$|m|$ state by absorption of microwave photons. The method has since been applied to other alkali metal atoms including cesium [1] and rubidium [13], and has been used to create continuous as well as pulsed beams of circular Rydberg atoms [14]. This technique employs the Stark effect to control the adiabatic microwave transfer. Because the Stark effect depends only on $|m|$, rather than m, both of the $\pm(n-1)$ states are equally populated. Consequently, the standard adiabatic microwave transfer method is not suitable for our application. Nussenzveig *et al.* [13] overcame this problem by applying a magnetic field to split the $\pm m$ degeneracy, working with rubidium.

Another method involves the excitation of a dressed state

*Present address: National Institute of Standards and Technology, Gaithersburg, MD 20899.

†Present address: Smithsonian Astrophysical Observatory, 60 Garden Street, Cambridge, MA 02138.

in the presence of a circularly polarized microwave field. The amplitude of the microwaves is reduced adiabatically, leaving the atoms in a particular circular state. This method, proposed by Molander *et al.* [15], was recently demonstrated by Cheng *et al.* in sodium [11]. However, efficient optical excitation of the initial state in a microwave field of modest amplitude requires either alkali-metal core-induced l mixing or an additional, static, electric field [16].

An entirely different approach to producing circular states was proposed by Delande and Gay [17]. This employs adiabatic switching of orthogonal electric and magnetic fields. In this ''crossed fields'' method, an $m=0$ Rydberg state is excited along a quantization axis that is then adiabatically redefined along a perpendicular axis for which $|m|=n-1$. The method was demonstrated by Hare *et al.* [12], who used an atomic beam of lithium that passed through spatially varying magnetic and electric fields, and was subsequently applied to rubidium [4] and barium [18].

In alkali-metal and other multielectron atoms, only the $m=+(n-1)$ state is easily accessible using the crossed fields method due to the effect of core perturbations on the initial states. In atomic hydrogen, however, this method allows selective preparation of either of the two circular states by starting from the highest or lowest $m=0$ Stark states. We have demonstrated this by using the crossed fields technique with two lasers tuned to the two different initial states. For this purpose, we developed a configuration of the crossed fields geometry that provides the rapid field switching necessary for a pulsed atomic source. This realization of the crossed fields method is described in Sec. II.

The crossed fields method worked efficiently, but ultimately proved cumbersome for our application. The circularizer had to be magnetically shielded, and the mechanical requirements this imposed compromised the radiative thermal design. Consequently, we developed a variant of the adiabatic microwave transfer technique, which requires no magnetic field. The new production region is part of an integrated system with all components in a cryogenic enclosure. This technique employs circularly polarized microwaves, rather than the usual linear polarization. By reversing the sense of rotation, the sign of m is reversed. This development is described in Sec. III.

II. THE CROSSED FIELDS METHOD

Delande and Gay showed [17], from SO(4) symmetry arguments, that a Rydberg atom can be transferred to a circular state by exciting it in a relatively strong electric field and a small perpendicular magnetic field, and then adiabatically switching off the electric field. We present here an equivalent description that provides somewhat more physical insight into the process and is helpful for determining the experimental requirements.

A. Angular momentum representation

In free space, the n^2 sublevels of the nth Rydberg manifold of hydrogen are degenerate. The orbital angular momentum $\vec{L}$ and the Runge-Lenz vector $\vec{A}$ are constants of motion. In an electric field, the degeneracy is partially removed and the angular momentum is no longer conserved. The states are naturally expressed in the parabolic representation with quantum numbers n, k, and m. If, instead, the system is quantized in an applied magnetic field, the states are naturally described in the spherical representation with quantum numbers n, l, and m. In the presence of both electric and magnetic fields the problem is not separable in either basis. However, as Pauli pointed out in 1926 [19], if the fields are small enough to neglect second-order effects, two quantities are conserved: the z components of the angular momentum and Runge-Lenz vectors, L_z and A_z. The angular-momentum-like quantization of the eigenvalues has been demonstrated experimentally by Penent *et al.* [20]. This basis provides a natural framework for describing dynamical processes in crossed electric and magnetic fields. We shall follow the notation of Demkov *et al.* [21].

Ignoring electron spin, the nonrelativistic Hamiltonian is (atomic units):

$$H=\underbrace{\frac{1}{2}P^2-\frac{1}{r}}_{H_0}+\underbrace{\frac{1}{2}\vec{B}\cdot\vec{L}}_{\text{Zeeman}}+\underbrace{\vec{F}\cdot\vec{r}}_{\text{Stark}}=H_0+W. \tag{1}$$

If second-order effects in the fields are neglected, the perturbation W is diagonal in a basis spanned by the angular-momentum-like operators $\vec{I}_1=\frac{1}{2}(\vec{L}+\vec{A})$ and $\vec{I}_2=\frac{1}{2}(\vec{L}-\vec{A})$. We begin by scaling the Runge-Lenz vector to the unperturbed Hamiltonian:

$$\vec{A}=(-2E_0)^{-1/2}\left[\frac{1}{2}(\vec{P}\times\vec{L}-\vec{L}\times\vec{P})-\hat{r}\right], \tag{2}$$

where E_0 is the eigenvalue of H_0. The perturbation becomes

$$W=-\frac{3}{2}n\vec{F}\cdot\vec{A}+\frac{1}{2}\vec{B}\cdot\vec{L}, \tag{3}$$

where we have made the Pauli replacement $\vec{r}\rightarrow-(3/2)n\vec{A}$. It is convenient to scale the fields to their relative perturbation strengths,

$$\vec{\mathcal{F}}\equiv\frac{3}{2}n\vec{F}\quad\text{and}\quad\vec{\mathcal{B}}\equiv\frac{1}{2}\vec{B}. \tag{4}$$

It can then be shown that, with these definitions and introducing

$$\begin{aligned}\vec{I}_1&\equiv\tfrac{1}{2}(\vec{L}+\vec{A}),\\ \vec{I}_2&\equiv\tfrac{1}{2}(\vec{L}-\vec{A}),\\ \vec{w}_1&\equiv-\vec{\mathcal{F}}+\vec{\mathcal{B}},\\ \vec{w}_2&\equiv\vec{\mathcal{F}}+\vec{\mathcal{B}},\end{aligned} \tag{5}$$

the perturbation takes the form

$$W=\vec{w}_1\cdot\vec{I}_1+\vec{w}_2\cdot\vec{I}_2. \tag{6}$$

The perturbation is diagonal in $|i_1,i_2\rangle$, where i_1 and i_2 are the projections of $\vec{I}_1$ and $\vec{I}_2$ onto $\vec{w}_1$ and $\vec{w}_2$, respectively.

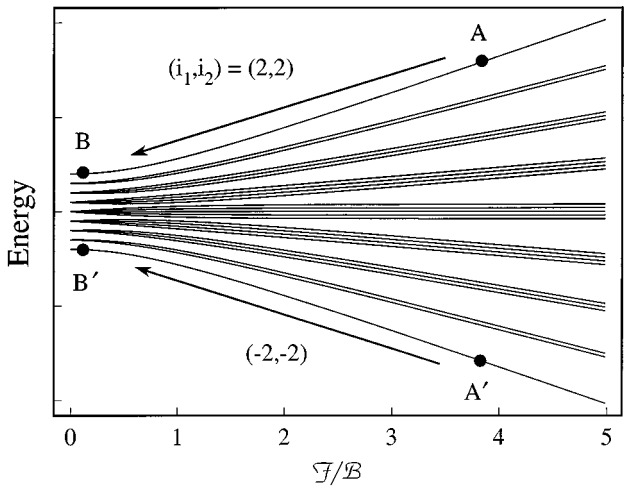

FIG. 1. Energy levels of the hydrogen $n=5$ manifold in nearly perpendicular electric and magnetic fields. The angle between $\mathcal{F}$ and $\mathcal{B}$ is $\pi/2+0.2$ rad. Arrows show the paths of adiabatic transfer. $\mathbf{A},\mathbf{A}'$: initial states. $\mathbf{B},\mathbf{B}'$: final, circular states.

The operators $\vec{I}_1$ and $\vec{I}_2$ have equal magnitudes and obey angular momentum commutation rules. Because $\vec{I}_1$, $\vec{I}_2$, and H_0 all commute we immediately have the eigenvalues of W [22]:

$$W=w_1 i_1+w_2 i_2, \tag{7}$$

where i_1,i_2 take on integer or half-integer values on the interval

$$-i_{\max}\leqslant i_1,i_2\leqslant i_{\max},$$

with $i_{\max}=\frac{1}{2}(n-1)$.

B. Adiabatic transfer to the circular state

We shall illustrate the principle of operation using the $n=5$ state of hydrogen for simplicity. The energy levels in nearly perpendicular electric and magnetic fields are shown in Fig. 1. In the Zeeman limit, where $\mathcal{F}\ll\mathcal{B}$, the highest and lowest states in the manifold are the circular states $|n,i_{\max},i_{\max}\rangle$ and $|n,-i_{\max},-i_{\max}\rangle$. These states are nondegenerate. The key to this method is that, in the Stark limit, where $\mathcal{F}\gg\mathcal{B}$, the $i_{1,2}=\pm i_{\max}$ levels are $m=0$ states which are accessible by laser excitation from low-lying states.

To produce circular states, the atoms are optically excited to one of the outermost Stark states in a region of strong electric field and weak perpendicular magnetic field (point **A** or $\mathbf{A}'$ in Fig. 1). The electric field is then slowly reduced to zero while the magnetic field is held constant. Atoms that follow the energy level adiabatically are transferred to a circular state (**B** or $\mathbf{B}'$, respectively).

The adiabaticity criterion can be obtained from simple vector arguments. As shown in Fig. 2, if $\vec{\mathcal{B}}$ is held constant while $|\vec{\mathcal{F}}|$ is reduced, $\vec{w}_2$ rotates and changes length. For $\vec{I}_2$ to follow $\vec{w}_2$ adiabatically, the rotation rate must always be slow compared to the precession rate, $\vec{w}_2\cdot\vec{I}_2$. The rotation rate of $\vec{w}_2$ is $\dot{\theta}=\mathcal{B}\dot{\mathcal{F}}/w^2$, where $\sin\theta\equiv\mathcal{B}/w$ and $w=\sqrt{\mathcal{F}^2+\mathcal{B}^2}$. The maximum rotation rate occurs at $\mathcal{B}\approx\mathcal{F}$,

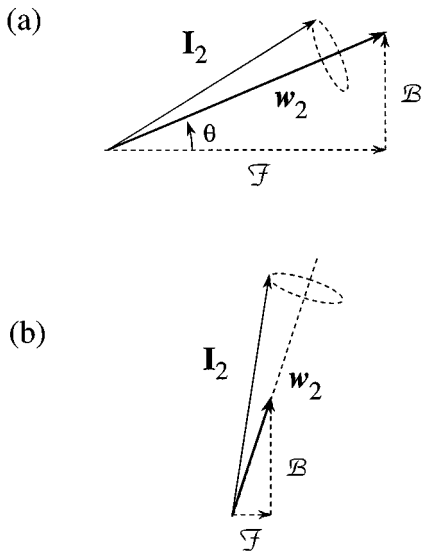

FIG. 2. Vector relationships for adiabatic transfer to the $m=n-1$ circular state. $\mathcal{B}$ is held constant while $\mathcal{F}$ is reduced. (a) $\mathcal{F}>\mathcal{B}$; (b) $\mathcal{F}<\mathcal{B}$.

and the adiabaticity condition becomes

$$\dot{\mathcal{F}}\ll 2\sqrt{2}\mathcal{B}^2, \tag{8}$$

or

$$\dot{F}\ll\frac{18B^2}{n}, \tag{9}$$

where $\dot{F}$ is in units of V/(cm μs) and B is in gauss. The same considerations apply to $\vec{w}_1$.

In this description the magnetic field is held constant while the electric field is changed but the method would also work with a constant electric field and time-varying magnetic field.

C. Diabatic return to Stark states

In the crossed fields method, the circular state is prepared defined relative to the applied magnetic field. For many experimental applications, including ours, the state must eventually be defined by an electric field. In principle this can be achieved by applying an electric field parallel to $\vec{B}$ and then allowing $\vec{B}$ to vanish. However, preserving the circular state in this process requires care.

The difficulty can be seen from Fig. 3, which displays energy levels in magnetic and electric fields that are nearly, but not exactly, parallel. Due to the misalignment there is a small perpendicular component of $\vec{\mathcal{F}}$, which produces an anticrossing when $\mathcal{F}\approx\mathcal{B}$. To remain in the circular state, this anticrossing must be traversed diabatically, moving from point **B** ($\mathbf{B}'$) to point **C** ($\mathbf{C}'$) in Fig. 3. Otherwise, the adiabatic process is reversed, and the atoms are restored to the $m=0$ state (points **D** and $\mathbf{D}'$).

The diabaticity criterion can also be found from the vector model, shown in Fig. 4. Here we consider the motion of the $\vec{I}_1$ vector, which initially precesses about the defining mag-

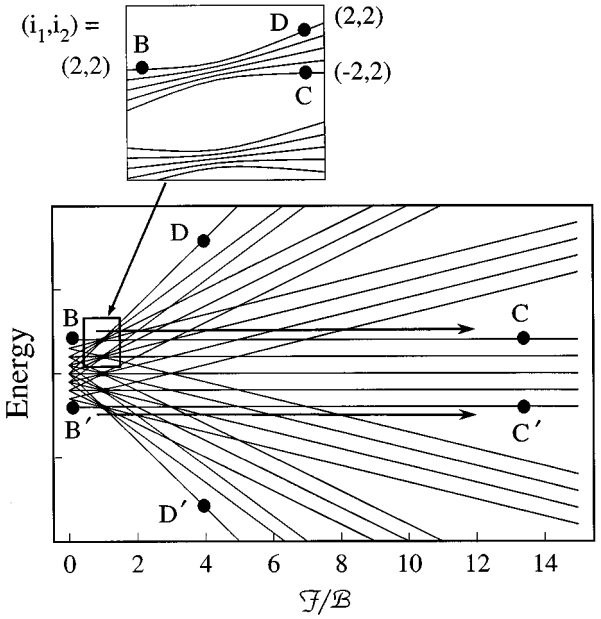

FIG. 3. Energy levels of the hydrogen $n=5$ in nearly parallel electric and magnetic fields. The angle between $\mathcal{F}$ and $\mathcal{B}$ is 0.1 rad. Note that the n-level anticrossing at $\mathcal{F}\approx\mathcal{B}$ would be an exact crossing for $\mathcal{F}\|\mathcal{B}$. Arrows show the paths for the diabatic redefinition of the circular states in an electric field. $\mathbf{B},\mathbf{B}'$: Circular states in magnetic field-dominated regime. $\mathbf{C},\mathbf{C}'$: Circular states in electric field-dominated regime. $\mathbf{D},\mathbf{D}'$: $m=0$ states produced if anticrossing is traversed adiabatically.

netic field $\vec{\mathcal{B}}$. As the parallel electric field is turned on, $\vec{w}_1=-\vec{\mathcal{F}}+\vec{\mathcal{B}}$ goes through a minimum and changes direction when $\mathcal{F}\approx\mathcal{B}$. If there is a small angular misalignment, δ, $\vec{w}_1$ rotates rapidly at this point instead of simply going through zero. It is essential to increase $\vec{\mathcal{F}}$ so rapidly that $\vec{I}_1$ is unable to follow $\vec{w}_1$, causing i_1 to change sign. The requirement for diabatic traversal is

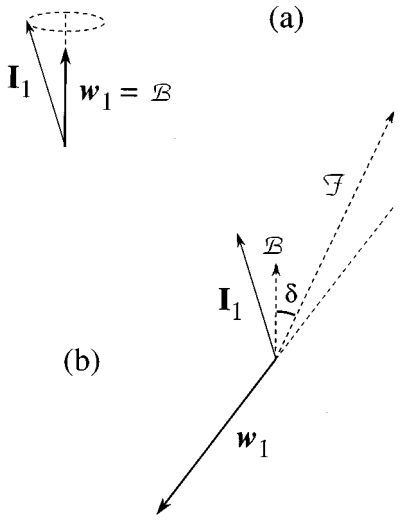

FIG. 4. Vector relationships for the diabatic switching of the $m=n-1$ circular state to the Stark basis. For clarity, the angular misalignment δ has been greatly exaggerated. (a) Initial condition, $\mathcal{F}=0$; (b) $\mathcal{F}>\mathcal{B}$.

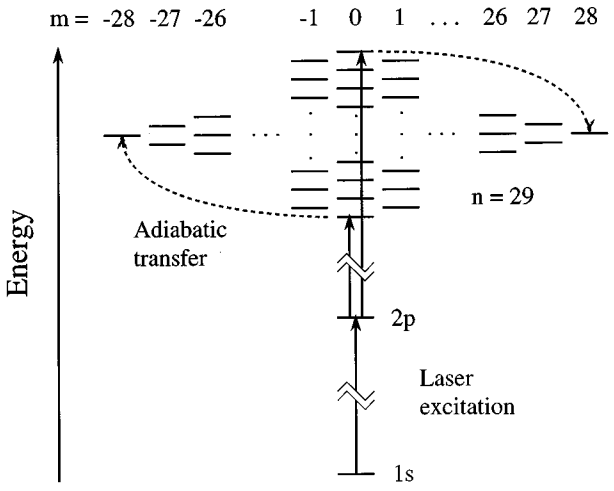

FIG. 5. Excitation scheme for circular state production in atomic hydrogen. Hydrogen atoms are elevated to one of the outermost Stark states by stepwise excitation through the $2p$ state. Subsequently, they are transferred to one of the two circular states.

$$\dot{\mathcal{F}}\gg\delta^2\mathcal{B}^2, \tag{10}$$

or

$$\dot{F}\gg\frac{6.4\delta^2B^2}{n}, \tag{11}$$

where $\dot{F}$ is in V /(cm μs) and B is in gauss.

D. Experiment

1. Excitation of $m=0$ Stark states

The excitation scheme for preparing $n=29$ circular states of hydrogen is illustrated in Fig. 5. The optical excitation requires 121.5 nm Lyman-α radiation to drive the $1s\rightarrow2p$ transition. Our laser system consists of two ultraviolet pulsed dye lasers, tunable around 365 nm. The first, tuned to 364.5 nm, is amplified to 10 mJ/pulse and focused into the center of a phase-matched krypton-argon gas mixture in which the third harmonic, at 121.5 nm, is generated by degenerate four-wave mixing [23]. The second dye laser, producing 1 mJ/pulse, drives the $2p\rightarrow$Rydberg transition at 366 nm.

2. Field switching

In previous implementations of the crossed fields method, the atoms drifted adiabatically out of the crossed fields region into a region of pure magnetic field [12,18,4]. This method is well suited to cw production, although it may not circularize the fastest atoms efficiently. Also, such spatial methods of adiabatic transfer in a thermal beam require a relatively long interaction region, particularly for a fast moving atom like hydrogen. Because our production technique is not cw but pulsed, we developed a pulsed device which avoids these difficulties.

The apparatus is illustrated in Fig. 6. A static magnetic field is applied perpendicular to the atomic beam. An electric field ($\vec{F}_A$) is applied parallel to the beam. Immediately following the optical excitation, the electric field $\vec{F}_A$ is turned

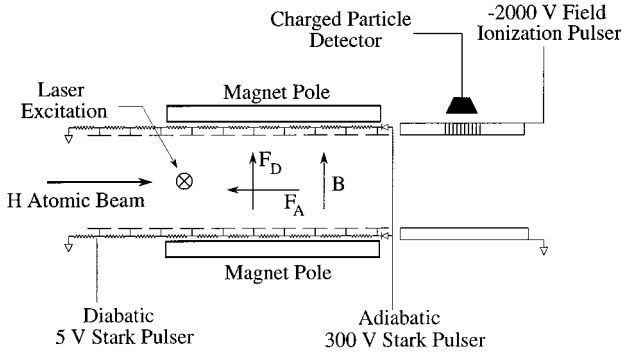

FIG. 6. Schematic of the circular state production region. The magnetic field is constant in the vertical direction. The UV and vacuum ultraviolet (VUV) lasers point into and out of the page and the hydrogen atoms travel from left to right. The electric field F_A is reduced to zero adiabatically; subsequently the electric field F_D is applied diabatically.

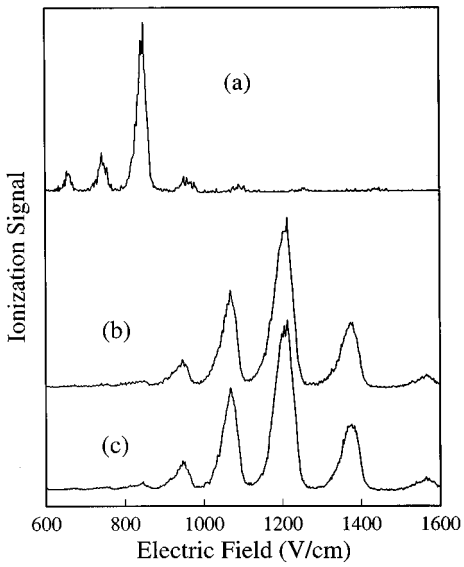

FIG. 7. Typical electric field ionization spectra for circular state production diagnosis. (a) One of the initial states, $|n=29,i_1=-28,i_2=-28,m=0\rangle$; (b) and (c) Circular states, $|n=29,i_1=28,i_2=-28,m=-28\rangle$ and $|n=29,i_1=-28,i_2=28,m=28\rangle$, respectively. Data were taken with a background temperature of 80 K. The circular state data have been scaled to the height of the initial state.

off adiabatically, and then an electric field $\vec{F}_D$ parallel to $\vec{B}$ is switched on rapidly. The adiabatic transfer and diabatic requantization occur within 10 μs of the laser excitation, before the excited volume can spread significantly due to velocity dispersion.

The magnetic field, $\approx$20 G, is produced by permanent magnets. The perpendicular electric field is produced by two arrays of metal strips connected by resistor chains. There are 40 pairs of strips along the 5 cm plate length, each pair located 0.5 cm above and below the atomic beam. Applying a voltage of 280 V to the resistor chain produces a field of $\approx$50 V/cm at the atomic beam. The field uniformity is better than 1% across the laser excitation volume. The requirement for adiabaticity, Eq. (9), yields

$$\dot{F}_A \ll 250 \text{ V/(cm } \mu\text{s)}. \tag{12}$$

The anticrossing occurs at $F_A=0.5$ V/cm, and Eq. (12) is easily satisfied by an exponentially decaying field with time constant $\tau \approx 1\,\mu$s.

The diabatic electric field $\vec{F}_D$ (parallel to $\vec{B}$) is applied to the strips uniformly, with no current flow through the resistor chain. For a worst case misalignment of the two fields ($\delta=0.1$ rad), the diabaticity criterion, Eq. (11), requires

$$\dot{F}_D \gg 1 \text{ V/(cm } \mu\text{s)}, \tag{13}$$

which is easily provided by a TTL-type pulser, which switches 0–5 V in 10 ns.

3. Signature of the circular states

Selective electric field ionization can be used to detect Rydberg atoms and to analyze their states. The threshold fields for ionization can be measured and the effectiveness of the angular momentum transfer process determined by analysis of the time-resolved ionization signal in the presence of a time-dependent ionizing field. However, the effectiveness of the adiabatic transfer process can also be demonstrated from relatively simple considerations.

The states in the n manifold with the lowest and highest ionization thresholds are the two initial states for circular state production, $|n,-i_{\max},-i_{\max}\rangle$ and $|n,i_{\max},i_{\max}\rangle$, respectively. The circular state threshold lies approximately midway between these two. Starting from the low-lying state, the threshold increases monotonically as the atom moves towards the circular state, while the reverse happens for an atom starting from the high-lying state. The paths lead to the $-(n-1)$ and $+(n-1)$ states, respectively, but since field ionization depends on $|m|$, not m, the two states ionize identically. When the process proceeds effectively, the two final states produce identical ionization signatures. Consequently, these are the circular states. Conversely, if transfer to each of the circular states is incomplete, the field ionization profiles for the two different paths will be different.

Field ionization spectra are shown in Fig. 7. The ionization signal for the initial state, the lowest Stark state, is shown in Fig. 7(a). (The highest Stark state is not displayed because its ionization field is too high for our detector.) Ionization profiles are shown for both the $m=-(n-1)$ and the $m=+(n-1)$ circular states, Figs. 7(b) and 7(c), respectively. The ancillary peaks in all three traces are neighboring states of nearby n populated by thermal transfer due to the 80 K background radiation in the apparatus. Note that in Fig. 7(b) there is virtually no trace of the initial $m=0$ state. We believe that the transfer process is close to 100% efficient.

III. ADIABATIC MICROWAVE TRANSFER

A. Principle of operation

To illustrate the principle of adiabatic microwave transfer, we again employ the $n=5$ manifold. Figure 8 shows the energy-level structure in an electric field with the relevant states now labeled by the parabolic quantum numbers (k,m). Initially, the atoms are in the lowest-lying state,

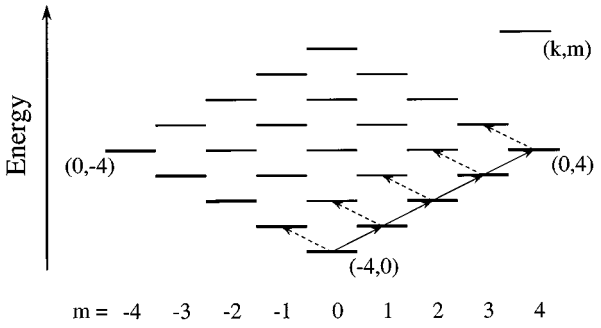

FIG. 8. Stark manifold for hydrogen $n=5$. The states are labeled with quantum numbers (k,m). Transitions leading to one of the circular states are shown with solid arrows. Leakage transitions are indicated with dashed arrows.

$|n,-(n-1),0\rangle$. The circular states lie at the left and right corners of the diagram, with quantum numbers $|n,0,-(n-1)\rangle$ and $|n,0,+(n-1)\rangle$, respectively.

Adiabatic microwave transfer takes place in a uniform electric field and circularly polarized microwave field. Initially, the electric field is large enough for the Stark splitting to exceed $\hbar\omega_m$, where ω_m is the microwave frequency. The electric field is then slowly decreased so that the Stark splitting passes through resonance. The population is transferred by adiabatic passage through $\Delta m=+1$ or $\Delta m=-1$ transitions, depending on whether the polarization is σ^+ or σ^-, respectively. After absorbing $n-1$ photons from the microwave field, the population is in either the $m=n-1$ or $m=-(n-1)$ circular state. Either circular state can be selected simply by changing the polarization of the microwave field.

The process may be pictured in the dressed atom representation, shown in Fig. 9. In this picture, the microwave coupling induces anticrossings at resonance. The atoms are initially prepared in the $m=0$ state **A**. If the Stark field is reduced through the anticrossing adiabatically, the population remains in the lowest-energy dressed state, absorbs $n-1$ photons, and emerges in state **B**, the circular state.

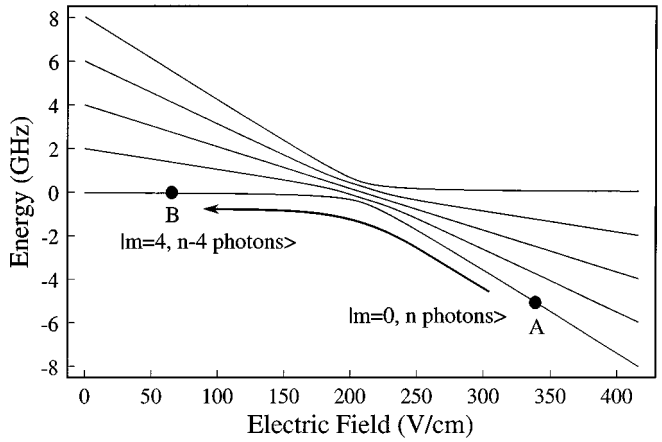

FIG. 9. The path to the circular state in the dressed state basis. Arrow shows the path of adiabatic transfer. At high electric field the lowest-energy state (**A**) is the $|m=0,n\text{photons}\rangle$ state. At low field, the lowest-energy state (**B**) is $|m=4,n-4\text{photons}\rangle$. Here the microwave field frequency is 2 GHz and the amplitude is 20 V/cm.

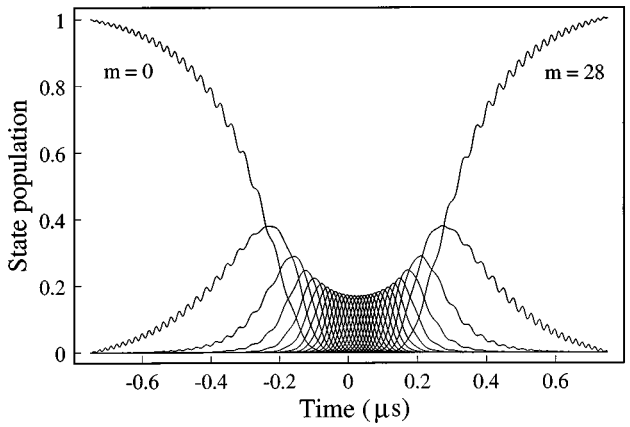

FIG. 10. Numerical simulation of transfer to the circular state. The state initially populated is $|n=29,k=-28,m=0\rangle$. Each of the 29 state populations along the path to the circular state is represented by a different solid line. The final population is almost completely in the $|n=29,k=0,m=28\rangle$ circular state.

In the first experimental demonstration of the adiabatic microwave transfer procedure [10], using the $n=19$ manifold in lithium, the second-order splittings exceeded the Rabi frequency. The system thus passed through a series of quasi-independent two-state anticrossings. In this case the probability for reaching the circular state can be obtained by repeatedly applying the Landau-Zener formula for each two-level system [10]. Denoting the Rabi frequency for the ith pair of coupled levels by ω_R^i and the (field-dependent) spacing of the levels by ω, then the probability of passing adiabatically through an avoided crossing is $1-\exp(-2\pi\gamma_i)$, where $\gamma_i=(\omega_R^i)^2/4\dot{\omega}$. The final population is determined by the product of the probabilities for each anticrosssing,

$$P_a=\prod_i (1-e^{-2\pi\gamma_i}).$$

In our experiment ($n=29$), however, second-order Stark splittings are small compared to the Rabi frequency. The transfer is fundamentally a multiphoton process in which many states are populated simultaneously. The parameter γ provides a useful figure of merit in choosing the experimental parameters, but for a quantitative analysis of the evolution of the state populations the Schrödinger equation must be integrated numerically.

Figure 10 displays a numerical simulation of the population transfer for the $n=29$ system, using parameters appropriate to our experimental conditions. The microwave field is assumed to have perfect σ^+ polarization. The microwave power is turned on and off with a sinusoidal pulse envelope. This adiabatic turn on substantially lowers the level of microwave power required for successful transfer.

The primary limitation to the efficiency of adiabatic microwave transfer is loss of population to ''leakage'' transitions such as those shown dashed in Fig. 8. With linearly polarized radiation, special steps must be taken to avoid leakage. In the initial demonstration of microwave adiabatic transfer [10], the applied electric field was sufficiently large to detune the leakage transitions due to the second-order Stark shift. However, for higher values of n this strategy no

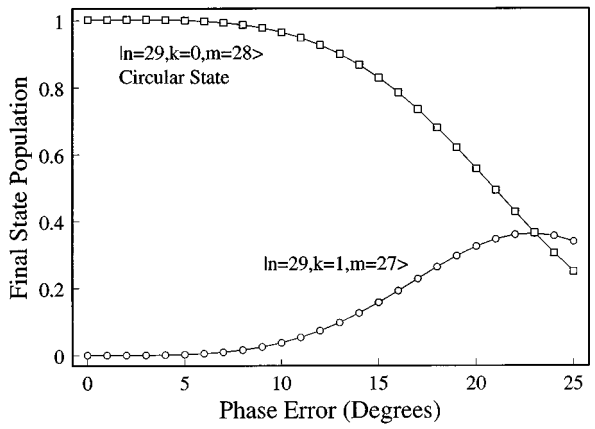

FIG. 11. Efficiency of circular state production vs phase error between the linear components of the microwave field. Zero phase error corresponds to perfect circular polarization. Squares: Final population in the $|n=29,k=0,m=28\rangle$ circular state after the adiabatic transfer. Circles: Final population in the neighboring $|n=29,k=1,m=27\rangle$ state.

longer works. Nussenzveig *et al.* produced $n=50$ circular states of rubidium by applying a small magnetic field to shift the leakage transitions off resonance [13]. The need for a magnetic field makes this technique unsuitable for our application. Instead, we employ a circularly polarized microwave field, which selectively drives only $\Delta m=+1$ or $\Delta m=-1$ transitions. Because of the simple structure of the hydrogen Stark manifold, either circular state can be populated from the same $m=0$ initial state depending on the sense of rotation of the applied field. However, good circular polarization is particularly important for the first few steps out of the initial state, where the leakage transitions are nearly or exactly (for the first step) degenerate with the desired transitions.

Because perfect circular polarization is difficult to achieve experimentally, we have studied the sensitivity of the transfer process to imperfect polarization. In Fig. 11 we plot the final circular state population as the ellipticity of the microwave field is increased. The parameters are the same as in Fig. 10, except that the phase angle between the linear components of the field is varied from 90° (0° phase error) to 65° (25° phase error). Ellipticity can also result from different amplitudes on the two components, but here the amplitudes are assumed equal. For phase errors up to 10°, more than 95% of the population goes to the circular state. Most of the remaining population ends up in the neighboring state $|n=29,k=1,m=27\rangle$, which does not interfere with our application.

B. Experiment

The apparatus for the circularly polarized adiabatic transfer method is illustrated in Fig. 12. The laser excitation to the $m=0$ initial state has been described in Sec. II D 1. The rotating microwave field is generated by two pairs of electrodes located at the corners of a 5 cm square. Each pair of electrodes constitutes the ends of a $3\lambda/2$ coaxial resonator with a Q of approximately 200. The resonators are driven in quadrature. The Stark field is applied symmetrically to the top and bottom plates. The electrodes are at a dc ground. The

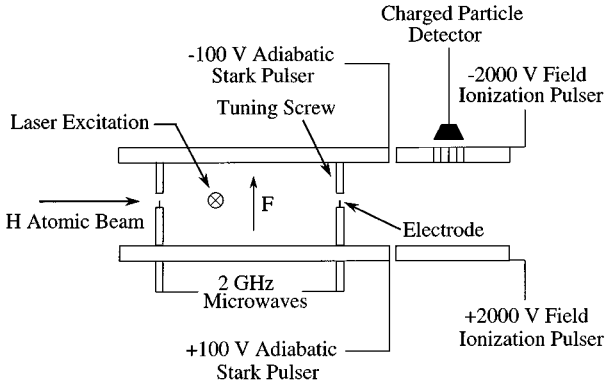

FIG. 12. Schematic of the adiabatic microwave transfer method production region. F is the Stark field. Two of the four microwave electrodes are visible in this side view.

symmetry of the geometry is improved by tuning screws, which also provide fine tuning of the frequency of the resonators by adding a variable capacitance to the electrodes.

The 2 GHz microwave pulse is shaped in a balanced mixer using a pulse generator with adjustable leading and trailing edges. A triangular control pulse produces an approximately sinusoidal power envelope. The quadrature drive signals to the two resonators are generated by a 90° power splitter, followed by a transfer switch that is used to reverse the polarization quickly. An adjustable delay in the lines allows fine tuning of the relative phase.

The time sequence for exciting the circular states is illustrated in Fig. 13. The atoms are optically excited in a field of 80 V/cm, at a point 2.5 mm before the center of the electrode array. Within 1 μs after the laser pulse, before the atoms have reached the center of the electrode array, the Stark field is rapidly reduced to 37 V/cm, leaving the state separation just above the resonance frequency. Then, as the atoms pass through the center of the electrode array, the transition is adiabatically swept through resonance with a Stark field slew rate of about 1 V/(cm μs). Simultaneously, the shaped pulse of the rotating microwave field is applied adiabatically.

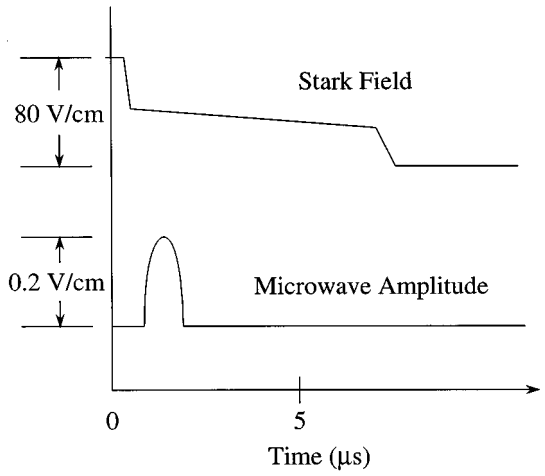

FIG. 13. Timing of the circular state production process. At $t=0$, the two-step laser excitation prepares a small volume of atoms in the $|n=29,k=-28,m=0\rangle$ state.

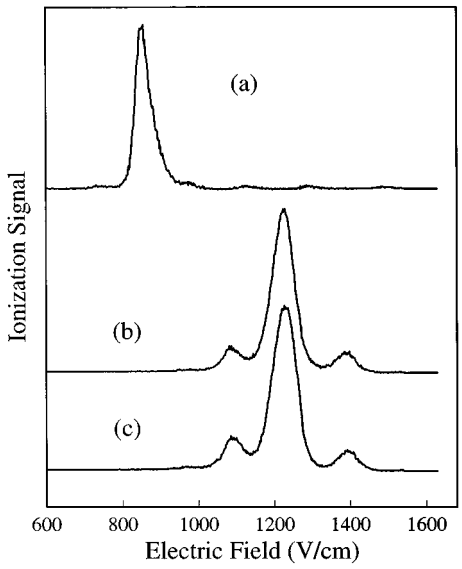

FIG. 14. Electric field ionization spectra for initial state and circular states prepared by the adiabatic microwave transfer method. (a) Initial state, $|n=29,k=-28,m=0\rangle$; (b) and (c) circular states, $|n=29,k=0,m=-28\rangle$ and $|n=29,k=0,m=28\rangle$, respectively. Data were taken with a background temperature of 10 K. The circular state data have been scaled to the height of the initial state.

Field ionization spectra for the $n=29$ initial state and the two circular states are shown in Fig. 14. The ionization signatures indicate that the atoms are efficiently transferred to the circular states. To understand the final state in detail we have carried out a study of the field ionization spectrum of the circular state.

C. Field ionization of circular states

Field ionization in hydrogen is fundamentally a tunneling process, where the ionization rate $\Gamma(F)$ for a given state increases extremely rapidly with increasing electric field. A 10% increase in field typically results in a 10^4-fold increase in Γ. Because of this behavior, for some purposes field ionization can be regarded as a simple threshold process. However, a careful analysis of the population of Rydberg atoms requires a detailed understanding of $\Gamma(F)$ for the states involved.

The Stark effect in hydrogen is exactly solvable and the wave function for any state can be numerically calculated, including the amplitude of the outgoing wave, and from such solutions $\Gamma(F)$ can be found. This technique, which yields what we shall call an exact solution, is numerically cumbersome. For many purposes, an analytic expression due to Damburg and Kolosov [24] can be employed. Their result, based on an extrapolation of an exact solution at low fields, is semiempirical. It is known to be accurate for states with low values of $|m|$ and large Stark shifts (i.e., large values of the parabolic quantum number $|k|$). However, for low values of $|k|$, it has been found to be in disagreement with exact calculations for hydrogen [25], and also experiments [26], raising doubts about its applicability to circular states.

Studies of field ionization of circular states of rubidium ($n=67,68$) [4], barium ($n=21$) [18], and sodium ($n=21$) [11] all report excellent agreement with the Damburg-Kolosov prediction. We have compared the predictions of the semiempirical formula with the results of exact calculations for $n=29$ states of hydrogen, carried out by Bergeman [25]. For the initial low-lying Stark state ($k=-28,m=0$), agreement is excellent over the range where $\Gamma(F)$ increases from $10^5\ \mathrm{s}^{-1}$ to $10^9\ \mathrm{s}^{-1}$, approximately 780 V/cm to 870 V/cm. For a given value of $\Gamma(F)$, the fields agree to within 0.5%.

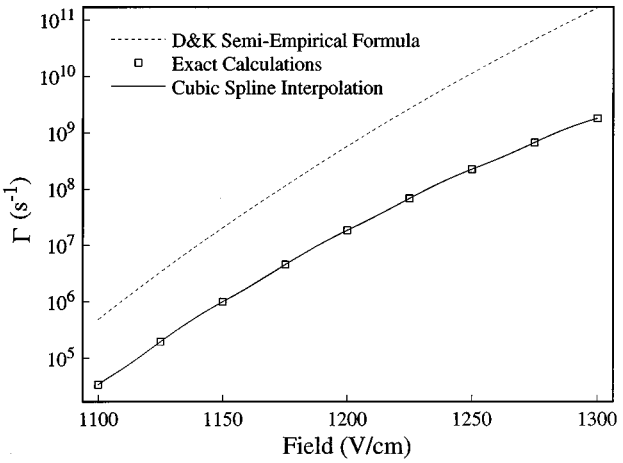

FIG. 15. Theoretical ionization rates for the circular state, $|n=29,k=0,|m|=28\rangle$. Dashed line: Damburg-Kolosov semiempirical formula. Squares: exact calculations. Solid line: cubic spline interpolation between the exact calculation points.

For the circular states, however, there is a systematic disagreement. As shown in Fig. 15, the fields for a given Γ can differ by as much as 8%. Alternatively, for a given field, values of $\Gamma(F)$ can differ by a factor up to 10^2. Over the entire range, the semiempirical formula yields values of $\Gamma(F)$ that are larger than those of the exact calculations.

Modeling the response of a pulsed field ionization detector to a population of atoms that have been excited and allowed to flow to the detector requires convolving the velocity distribution of the beam with the electric field profile in the ionizer and the temporal profile of the rising field. The modeling must be carried out with care because of the extreme sensitivity of Γ to F and to the atom motion during the ramp time of the pulser. The results of such a study [27] are shown in Fig. 16. The excellent agreement of the experimental data with both the exact calculation [25] and the semiempirical formula for the initial Stark state, $|n=29,k=-28,m=0\rangle$, gives confidence that the modeling was carried out accurately. For the circular state, the exact calculation and experiment are in good agreement, although the width of the observed signal is slightly larger than predicted. The semiempirical formula, however, reveals a profile shifted significantly to shorter time. This corresponds to ionizing at a lower field, as is to be expected if the predicted value of $\Gamma(F)$ is higher than the actual value.

IV. MILLIMETER-WAVE RESONANCE WITH CIRCULAR STATES OF HYDROGEN

As mentioned in the Introduction, our goal in creating circular states in hydrogen is to determine the Rydberg fre-

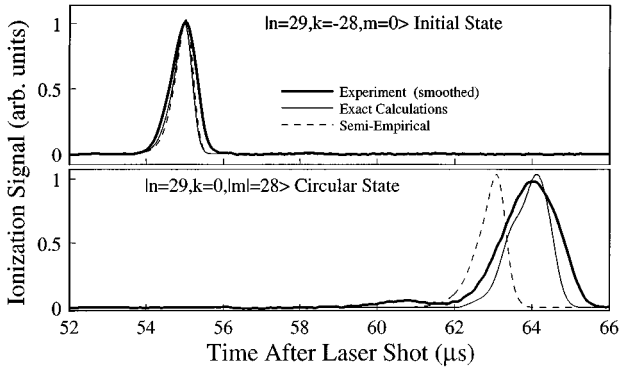

FIG. 16. Field ionization signal for the initial state, $|n=29, k=-28, m=0\rangle$, and the circular state, $|n=29, k=0, |m|=28\rangle$. Dashed line: Damburg-Kolosov semiempirical formula. Solid line: exact calculations. Heavy line: experimental data (smoothed).

quency cR_H by measuring the transition frequency between the $n=29$ and $n=30$ circular states, at ≈ 256 GHz. In addition to contributing to the precision measurement of cR_H, spectroscopy of the circular states provides a valuable diagnostic on the effectiveness of the circular state production process.

In the simplest experimental geometry, a beam of $n=29$ circular state atoms, produced by adiabatic microwave transfer, travels through the Gaussian focus of a millimeter-wave beam. A state-sensitive electric field ionization detector records the final populations of the $n=29$ and $n=30$ states as the millimeter-wave frequency is tuned through the atomic resonance frequency. The entire apparatus is magnetically shielded and cryogenically cooled to a radiation temperature of 10 K. The experiment operates at 30–60 pulses per second, and the arrival time of the atoms is recorded along with the state distribution. A typical signal rate is 100 circular atoms per pulse at the end of the apparatus.

The population inversion is computed from the normalized difference of the detected populations, given by

$$\mathcal{I}=\frac{N_{30}-N_{29}}{N_{30}+N_{29}}, \tag{14}$$

where N_{30} and N_{29} are the numbers of detected ions from the $n=30$ and $n=29$ circular states, respectively. A velocity-averaged experimental resonance curve is shown in Fig. 17. The measured linewidth is 80 kHz full width at half maximum (FWHM), compared with the 70 kHz transform limit of the distribution of interaction times.

This ''Rabi resonance'' technique, with inherent precision of ≈ 100 KHz, may be used to analyze the populations of high-$|m|$ states, with $|m|<n-1$, resulting from incomplete transfer and leakage transitions. The most likely candidate is the $|k=1,|m|=n-2\rangle$ state, which is not easily resolved from the circular state by electric field ionization. The relative population of the $|k=1,|m|=n-2\rangle$ state can be measured by comparison of the inversion amplitude of the $|n,k=1,|m|=n-2\rangle \rightarrow |n+1,k=1,|m|=n-1\rangle$ transition with that of the circular-circular transition. In an electric field of 1 V/cm, these transitions are separated by 1.9 MHz and are easily resolved. Such a measurement has been used to verify that the accidental population of the $|m|=n-2$ state is less than 5% of the circular state population.

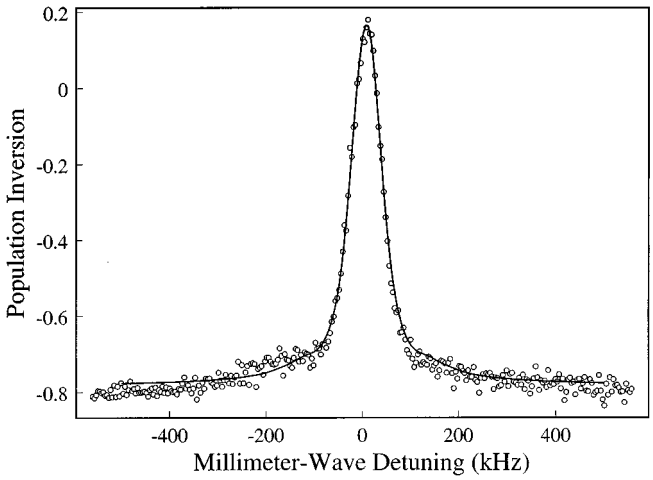

FIG. 17. Rabi resonance curve resulting from interaction with one of the millimeter-wave fields. Open circles: experimental data. Solid line: fit of the Rabi line shape to the data. The millimeter-wave waist size and power were free parameters in this fit.

For maximum experimental resolution and precision, the experiment employs the separated oscillatory field geometry (''Ramsey resonance'') [28]. After passing through the first resonance region, the atomic beam travels 50 cm and passes through a second focused millimeter-wave beam. This arrangement provides increased precision without additional line broadening from time- and spatially varying perturbations. The resolution with separated millimeter-wave fields is approximately 1 kHz.

A pair of velocity-averaged Ramsey curves taken under similar conditions is shown in Fig. 18. The curves were taken for the two circular-circular transitions, $\Delta m=+1$ and $\Delta m=-1$. The shift in their central frequencies, about 400 Hz, is due to the Zeeman effect in a residual field of about 140 μG. These data were taken with a deuterium beam, which gives better fringe contrast than hydrogen for some

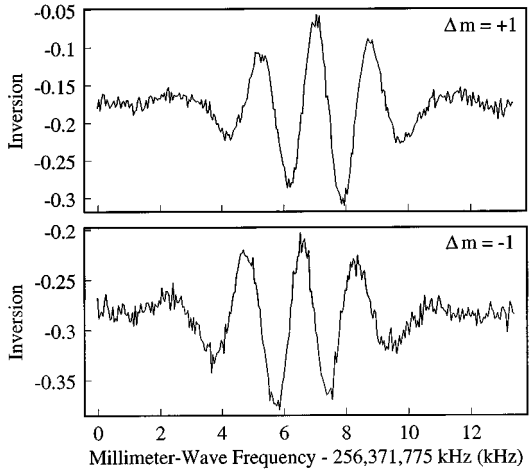

FIG. 18. Ramsey curves for the two circular-circular transitions in deuterium, $\Delta m=+1$ and $\Delta m=-1$. The frequency shift between the two curves corresponds to an average magnetic field of 140 μG.

beam temperatures. The linewidth of 850 Hz is in good agreement with the theoretical predictions. The shift in the line position on reversing the 2 GHz polarization is clear evidence that we are producing each circular state selectively.

V. CONCLUSION

We have demonstrated the production of circular states of hydrogen by adiabatic transfer in crossed electric and magnetic fields and also by adiabatic passage in a circularly polarized microwave field. Both methods have been shown to be efficient.

The effectiveness of the transfer processes has been verified both by electric field ionization and by high-precision spectroscopy of transitions between the $n=29$ and $n=30$ circular states. Theoretical line shape calculations are in good agreement with our experimental results. These techniques and measurements lay the groundwork for a precision measurement of the Rydberg constant in hydrogen.

ACKNOWLEDGMENTS

The authors thank Dr. Thomas Bergeman for calculating the ionization rates of the initial and circular states. This research was supported by the Joint Services Electronics Program and the National Science Foundation.

[1] R. G. Hulet, E. S. Hilfer, and D. Kleppner, Phys. Rev. Lett. **55**, 2137 (1985).
[2] M. Brune, P. Nussenzveig, F. Schmidt-Kaler, F. Bernardot, A. Maali, J. M. Raimond, and S. Haroche, Phys. Rev. Lett. **72**, 3339 (1994).
[3] M. Brune, E. Hagley, J. Dreyer, X. Maitre, A. Maali, C. Wunderlich, J. M. Raimond, and S. Haroche, Phys. Rev. Lett. **77**, 4887 (1996).
[4] R. J. Brecha, G. Raithel, C. Wagner, and H. Walther, Opt. Commun. **102**, 257 (1993).
[5] J. Liang, M. Gross, P. Goy, and S. Haroche, Phys. Rev. A **33**, 4437 (1986).
[6] J. Hare, A. Nussenzweig, C. Gabbanini, M. Weidemuller, P. Goy, M. Gross, and S. Haroche, IEEE Trans Instrum. Meas. **42**, 331 (1993).
[7] R. Lutwak, J. Holley, J. DeVries, T. Ducas, and D. Kleppner, in *Proceedings of the Fifth Symposium on Frequency Standards and Metrology*, edited by J. C. Bergquist (World Scientific, Singapore, 1996), p. 259.
[8] S. B. Hansen, T. Ehreneich, E. Horsdal-Pedersen, K. B. MacAdam, and L. J. Dube, Phys. Rev. Lett. **71**, 1522 (1993).
[9] M. P. deBoer, J. H. Hoogenraad, R. B. Vrijen, L. D. Noordam, and H. G. Muller, Phys. Rev. Lett. **71**, 3263 (1993).
[10] R. G. Hulet and D. Kleppner, Phys. Rev. Lett. **51**, 1430 (1983).
[11] C. H. Cheng, C. Y. Lee, and T. F. Gallagher, Phys. Rev. Lett. **73**, 3078 (1994).
[12] J. Hare, M. Gross, and P. Goy, Phys. Rev. Lett. **61**, 1938 (1988).
[13] P. Nussenzveig, F. Bernardot, M. Brune, J. Hare, J. M. Raimond, S. Haroche, and W. Gawlik, Phys. Rev. A **48**, 3991 (1993).
[14] A. Nussenzweig, J. Hare, A. M. Steinberg, L. Moi, M. Gross, and S. Haroche, Europhys. Lett. **14**, 755 (1991).
[15] W. A. Molander, C. R. Stroud, Jr., and J. A. Yeazell, J. Phys. B **19**, L461 (1986).
[16] L. Chen, M. Cheret, F. Roussel, and G. Speiss, J. Phys. B **26**, L437 (1993).
[17] D. Delande and J. C. Gay, Europhys. Lett. **5**, 303 (1988).
[18] M. Cheret, F. Roussel, T. Bolzinger, G. Spiess, J. Hare, and M. Gross, Europhys. Lett. **9**, 231 (1989).
[19] W. Pauli, Z. Phys. **36**, 336 (1926).
[20] F. Penent, D. Delande, F. Biraben, and J. C. Gay, Opt. Commun. **49**, 184 (1984).
[21] Yu. N. Demkov, B. S. Monozon, and V. N. Ostrovskii, Zh. Eksp. Teor. Fiz. 57, 1431 (1969) [Sov. Phys. JETP **30**, 775 (1970)].
[22] There is a disagreement in the published literature on the assignment of quantum numbers to the angular momenta $\vec{I}_1$ and $\vec{I}_2$. For comparison with the parabolic basis (n,k,m), it is convenient to quantize i_1 and i_2 along the electric field axis [21], so that $W=i_1w_1-i_2w_2$. For describing the dynamical behavior in changing electric and magnetic fields we find that it is more illuminating to quantize $\vec{I}_1$ and $\vec{I}_2$ along $\vec{w}_1$ and $\vec{w}_2$, respectively, as we have done in Eq. (7).
[23] See, for example, R. Hilbig, G. Hilber, A. Lago, B. Wolff, and R. Wallenstein, Comments At. Mol. Phys. **18,** 157 (1986), and references therein.
[24] R. J. Damburg and V. V. Kolosov, J. Phys. B **12**, 2637 (1979).
[25] T. Bergeman (private communication).
[26] P. M. Koch and D. R. Mariani, Phys. Rev. Lett. **46**, 1275 (1981).
[27] R. Lutwak, Ph.D. thesis, Massachusetts Institute of Technology, 1996.
[28] N. F. Ramsey, *Molecular Beams* (Oxford University Press, New York, 1956), pp. 124–144.